Macromolecules
COMMUNICATION TO THE EDITOR

*Macromolecules* **2009**, *42*, 8017–8020 **8017**
DOI: 10.1021/ma901220c

# Binaphthalene-Based, Soluble Polyimides: The Limits of Intrinsic Microporosity

**Nicola Ritter,[†] Markus Antonietti,[†] Arne Thomas,[†] Irena Senkovska,[‡] Stefan Kaskel,[‡] and Jens Weber*,[†]**

[†]*Max Planck Institute of Colloids and Interfaces, Dept. of Colloid Chemistry, Research Campus Golm, D-14424 Potsdam, Germany, and* [‡]*Department of Inorganic Chemistry, Dresden University of Technology, Mommsenstr. 6, D-01069 Dresden, Germany*

*Received June 8, 2009*
*Revised Manuscript Received September 28, 2009*

Microporous, purely organic materials gained increasing interest during the past years as they have a high potential in a variety of applications like gas separation or storage.[1] Because of recent synthetic advances, there is a broad structural variety of cross-linked microporous polymers, as there are for instance poly(benzodioxane)s,[2] poly(imide)s,[3] poly(aniline)s,[4,5] various conjugated polymers,[6−8] poly(organosilanes),[9] poly(arylcarbinols),[10,11] and hyper-cross-linked resins.[12] This pool of polymer architectures is complemented by regular frameworks, covalent organic frameworks that are based on boron−oxygen or triazine systems.[13,14]

On the other hand, there is a great interest in soluble, microporous polymers (which are consequently non-cross-linked), as they are much easier to process. However, only a very limited number of microporous, soluble polymers are known up to now. The most prominent examples are the polymers of intrinsic microporosity (PIM)s, which were introduced by Budd et al. recently.[15] They feature a 90° kink in every repeat unit of the otherwise stiff ladder-type poly(benzodioxane)s. This kink prohibits the space-efficient packing of the polymer chains and leads to a large, interconnected amount of free volume. This free volume is accessible to probe molecules as for instance nitrogen, and the polymers are therefore considered to be microporous.[16] In a former communication, we showed that the principle can be expanded on soluble poly(imide) using spirobifluorene as the building block.[17]

In the present study we investigate the use of (±)-2,2′-diamino-1,1′-binaphthalene (**1**) as a monomer for the synthesis of soluble, microporous poly(imide). The use of binaphthalene derivatives as monomers for PIMs was suggested already by Budd and McKeown and investigated in more detail just recently by Guiver and co-workers.[15,18] However, no detailed investigation of the porosity of such systems by means of gas sorption was presented yet. Herein, we show a detailed analysis of the gas sorption behavior of binaphthalene-based poly(imide), employing nitrogen, hydrogen, and carbon dioxide as sorbates.

Figure 1 shows the chemical structure of **1** and the corresponding poly(imide), which is obtained by reaction of **1** with benzene-1,2,4,5-tetracarboxylic anhydride (**2**) together with the spatial structure of **1**.

Polyimides were prepared by two different pathways. First, a one-step route, employing *m*-cresol as solvent and isoquinoline as catalyst, was used. **1** and **2** were dissolved in *m*-cresol in equal amounts under a $N_2$ atmosphere. After the dissolution of the monomers, isoquinoline is added and the mixture is stirred for 1 h. Then it is first heated at 80 °C for 2 h and then at 200 °C for 6 h. The resulting polyimide usually shows a weight-average molecular weight ($M_w$) of about 5000 g/mol as determined by GPC.

The second way of producing the polyimide is a two-step reaction in which first a polyamic acid is formed, which is then further condensed to a polyimide. The polyamic acid is formed by reacting equal amounts of **1** and **2** in dry NMP under a $N_2$ atmosphere and stirring it overnight. The polyamic acid is precipitated, vacuum-dried at 40 °C, and cured for 2 h at 300 °C in a $N_2$ atmosphere. The crude polyimide usually had a $M_w$ of about 8000 g/mol. Generally speaking, higher molecular masses were obtained via the polyamic acid route. A further advantage of this reaction design is the use of less toxic and hazardous solvents and catalysts.

The resulting polymers were soluble in $CHCl_3$, DMSO, NMP, THF, DMAc, and DMF. The easy solubility in less interacting solvents like THF or $CHCl_3$ can already be ascribed to the contorted structure of the polyimide. Molecular weights and molecular weight distributions were determined by gel permeation chromatography (GPC) against PMMA standards (see Figure 2). The data obtained by GPC have to be discussed with care since the chemical and structural composition of the used standard PMMA differs significantly from the analyte, but gives nevertheless an estimate.

The molecular weight distributions were generally moderate (PDI ∼ 2.5). Nevertheless, the polymer was fractionated using selective precipitation in a chloroform/ethanol mixture. The original product showed a shoulder at an elution volume of about 12.2 mL. Surprisingly, we found this shoulder which belongs to a relatively low molecular weight compound again as a pronounced peak in the first fraction. The following fractions however followed the laws of polymer fractionation, i.e., higher molecular weight polymers formed the early fractions, while the later fractions were composed mainly out of lower molecular weight polymers or oligomers. Figure 2 shows the corresponding GPC traces. On the basis of preliminary MALDI-TOF analysis, we speculate that the compound responsible for the shoulder and the peak at 12.2 mL is a cyclic product (see Figure S1). The formation of cyclic byproducts is not uncommon for PIMs.[19−21] However, we cannot discuss these byproducts in full detail at this stage and will therefore concentrate on the later fractions solely.

The fractions were further analyzed by means of nitrogen and hydrogen sorption as well as wide-angle X-ray scattering (WAXS). Their chemical identity was verified by infrared spectroscopy. WAXS measurements confirmed the amorphous nature of the polymers.

Initial analysis of the sample porosity was performed using nitrogen sorption at 77 K. Specific surface areas were calculated using the BET approach. Typical nitrogen sorption isotherms obtained from samples precipitated from chloroform into ethanol (ratio 1:3), in the following annotated as *precipitated* samples, are depicted in Figure 3.

Typically, a low nitrogen uptake at low relative pressures was observed, which results in low specific surface areas. At higher relative pressures, there is a significant uptake of nitrogen, which is due to the condensation of nitrogen in the voids between the precipitated polymer particles. The presence of this microparticulate structure is also responsible for the determined BET surface area. In conclusion, the nitrogen sorption measurements indicated that the samples were not microporous.

*Corresponding author: fax +49-331-5679502, ph +49-331-5679569, e-mail jens.weber@mpikg.mpg.de.


Published on Web 10/09/2009

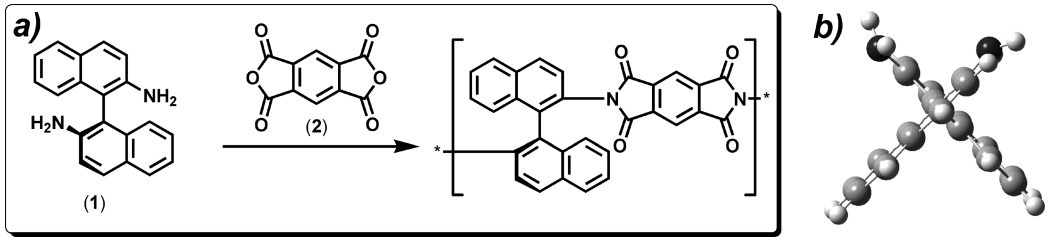


**Figure 1.** (a) Chemical structures of the monomers **1** and **2** and the resulting polyimide. (b) Model of the spatial structure of **1**.

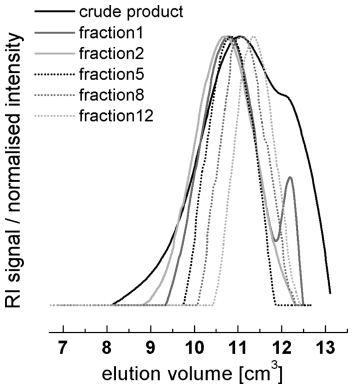


**Figure 2.** GPC traces (standard PMMA in DMSO) for the crude polymer and its fractions.

It should be noted that a huge low-pressure hysteresis (up to 100 $cm^3\ g^{-1}$) upon desorption was observed in some cases (Figure S2). It is known that nitrogen might swell the pores and can interact strongly with the polymer.[3] It was also reported that nitrogen sorption measurements on PIM-polyimides can last up to 380 h.[22] Furthermore, gas sorption experiments on activated carbons showed that the diffusion of nitrogen into very narrow pores might be infinitely slow because of the low kinetic energy of nitrogen at 77 K.[23] This effect might be also active for the polyimides under investigation. This is one reason while the sorption of hydrogen at 77 K, a temperature well above its critical point, can be regarded as a more appropriate analytical tool for microporous polymers.[4] It was shown for hyper-cross-linked polyaniline and PIM-type polyamide that hydrogen might enter (and therefore screen) pores that are inaccessible for nitrogen.[3,5] Moreover, carbon dioxide sorption at 273 K was also shown to be a versatile analytical tool for the analysis of microporous materials with very narrow pores that cannot be accessed by nitrogen.[23,24] This molecular-sieving type behavior is already known for some activated carbons and metal−organic frameworks (MOFs)[23,25,26] but has rarely been reported for amorphous polymers.

Analysis of the samples precipitated from chloroform by means of hydrogen and carbon dioxide sorption indeed showed that the samples adsorb significant amounts of these gases (Figure 3). It should be noted that the sorption isotherms of $H_2$ and $CO_2$ cannot be compared directly to that of $N_2$ as the conditions were too different.[27]

Interestingly, we observed a significant hysteresis upon desorption of hydrogen and carbon dioxide. This hysteresis can have various origins. First, it is possible that the polymer changes its morphology as a consequence of the increasing gas pressure or condensation within the pores. This effect would be in accordance with observations of structural changes upon helium adsorption in microporous polymer networks at room temperature.[3] Such behavior might be in accordance with reports on hydrogen sorption hysteresis in flexible metal−organic frameworks.[28−30] Second, we cannot exclude kinetic effects as described for the adsorption of hydrogen in ultramicropores.[5] These kinetic effects may just arise from very small pores adapting their size to fit exactly that of hydrogen or carbon dioxide molecules.

It is possible to calculate specific surface areas from the hydrogen sorption measurements using the Langmuir approach. The specific surface areas were calculated to be in the range of 150−170 $m^2\ g^{-1}$, which is in accordance with reports on microporous polymers of comparable $H_2$ uptake.[3,5] However, extreme care has to be taken when discussing the derived values as certain side assumptions have to be considered.[31] Nevertheless it is possible to state that the detected difference in the sorption behavior of the materials with regard to nitrogen and carbon dioxide or hydrogen could be explained by the inability of nitrogen molecules to diffuse in very small pores. In contrast, $H_2$ and $CO_2$ have a smaller kinetic diameter as well as a higher kinetic energy and can in fact enter these pores.

It was shown in former work that there is an influence of the processing on the observable porosity.[17] Spirobifluorene-based polyimide was shown to be microporous if precipitated from chloroform but not if precipitated from more strongly interacting solvents such as DMAc or DMF. Hence, we were interested if such effect holds true also for the polyimide under investigation. We measured the hydrogen and carbon dioxide sorption of samples, which were cast from solutions of the polymer in chloroform and DMSO, respectively.[32] It turned out that none of these samples showed a significant uptake of hydrogen. Pore blocking by trapped solvent molecules could be excluded based on spectroscopic and thermogravimetric analysis (see Figures S6−S9).

However, the solvent cast films were able to adsorb significant amounts of carbon dioxide, though in less amounts than the precipitated samples (~1 mmol $g^{-1}$, see Figure S3). Given the fact that the kinetic diameter of $H_2$ ($d$ = 2.89 Å) is smaller than that of $CO_2$ ($d$ = 3.3 Å), it is obvious that the system does not discriminate solely on molecular-sieving effects but also on polymer−penetrant interactions. As carbon dioxide has a significant quadrupolar moment, its interaction with the highly polar imide functionalities cannot be neglected. Indeed, it is known that some polyimide membranes are sensitive to $CO_2$ plasticization and are known to adsorb $CO_2$ even at low pressures.[33−35]

Comparative analysis of the samples (precipitated and solvent cast) by WAXS also showed remarkable differences depending on the processing as shown in Figure 4. Two main features can be identified in all patterns. First, there is a rather well-defined reflection at $2\theta \sim 11°$. This reflection corresponds to a $d$-spacing of ~8 Å. This value is related to the average distance of the imide linkage between two binaphthalene units[36] but presumably (due to electron density arguments) reflects to the distance between only loosely packed chains, i.e., the amorphous repeat period between micropores.[17] The second common feature is a broad peak at ~19°−20° (corresponding to a $d$-spacing of ~4.5 Å), which is typical for all densely packed amorphous polymers and usually attributed to the average chain−chain distance. It is now observed that the ratio between those two peaks is dependent on the processing. If the polymers are precipitated from $CHCl_3$,

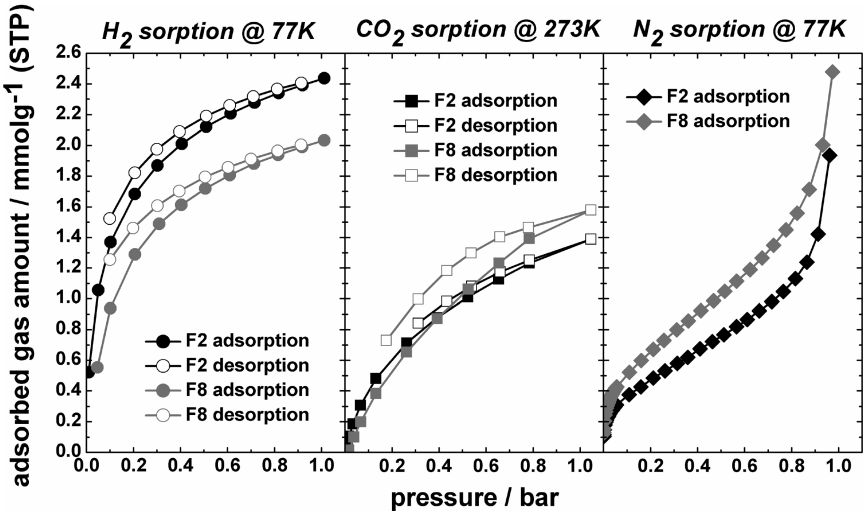


**Figure 3.** Hydrogen sorption isotherms at 77 K (left-hand side), carbon dioxide sorption isotherms at 273 K (middle), and nitrogen adsorption isotherms (right-hand side) of fractions F2 and F8; closed symbols: adsorption; open symbols: desorption.

**Table 1. Molecular Weight (Weight Average), Polydispersity, Specific Surface Areas, and Maximum Hydrogen and Carbon Dioxide Uptake at 1 bar of Two Precipitated Polyimide Fractions**

| sample | $M_w$ [g/mol] | PDI | $S_{BET}$[a] [$m^2$/g] | $S_{Langmuir}$[b] [$m^2$/g] | $H_2$ uptake[c] [wt %] | $CO_2$ uptake[d] [mmol $g^{-1}$] |
|---|---|---|---|---|---|---|
| F2 | 11000 | 1.68 | 40 | 171 | 0.5 | 1.39 |
| F8 | 6000 | 1.41 | 57 | 149 | 0.45 | 1.58 |

[a] Determined by applying the BET model to nitrogen adsorption isotherms at 77 K. [b] Determined by applying the Langmuir model to hydrogen adsorption isotherms at 77 K. [c] At 77 K and 1 bar. [d] At 273 K and 1 bar.

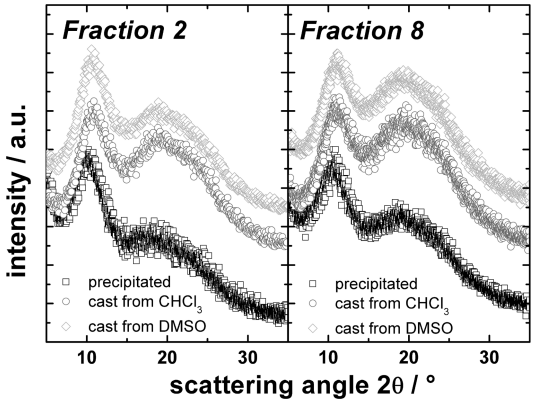


**Figure 4.** Wide-angle X-ray scattering patterns of polyimide fractions F2 and F8, which were precipitated from chloroform (squares), solvent cast from chloroform (circles), or solvent cast from DMSO (rhombi).

the peak at ~20° has a lower intensity. When the polymers were solvent cast, the intensity of that broad peak is increased, while the 11° peak is significantly lowered. Hence, the packing and density of the sample are different on the molecular level. This result can be read as an indirect proof of the existence of a metastable state when precipitated on which the sample contains trapped intrinsic microporosity. When solvent cast, the (solvent swollen) polymer chains are obviously free to assemble into a more closely packed glass, which does not allow easy access for small guest molecules. It is a general rule of solid state thermodynamics that phases with higher density also have a lower free energy; i.e., we consider the dense film state as thermodynamically more stable.

Table 1 summarizes the results obtained on two fractions of the binaphthalene-based polyimide.

In conclusion, we have shown that ultramicroporous polyimide can be prepared, employing racemic 2,2′-diamino-1, 1′-binaphthalene. The resulting polyimide showed, contrary to other polyimides, good solubility in a broad variety of organic solvents, which can be attributed to its contorted structure which suppress easy, space-efficient packing.

The porosity of the samples was however only reflected in their ability to adsorb significant amounts of hydrogen or carbon dioxide, showing that the analysis of (potentially) microporous polymers requires more than one method in order to acquire a more complete picture. It could further be shown that the microporosity was dependent on the processing. If precipitated from a good solvent into a nonsolvent, a metastable state of microporosity was "frozen" in which was even kept throughout all further sorption experiments. When the polymers were however film processed from a good solvent, no or less accessible microporosity was observed; that is, even the highly contorted binaphthalene structures were able to be packed into a dense film. It is an open question if this is peculiar for the presented polyimide which then can be regarded as an intermediate between "classic" PIMs and polymers of high free volume. However, it is also possible that all linear contorted polymers are still able to pack, appropriate time scales and mobility assumed, making this question to it a very interesting subject of polymer physics and simulation.

The molecular weights of the polymers presented here were only moderate. This is in accordance with reports on other PIMs based on binaphthalene units[18] but hampers the production of mechanically stable, tough films which will be needed to test the polymers for their performance in gas separation processes. As we have high expectations for such applications, future work will concentrate on the optimization of the synthesis conditions as well as on the investigation of the highly defined cyclic byproducts, which are by definition "polymerizable pores".

**Acknowledgment.** We thank Marlies Gräwert (MPIKG) for GPC measurements. Dr. Niklas Hedin and Dr. Zoltan Bacsik (Stockholm University) are acknowledged for discussion of the carbon dioxide sorption experiments. Financial support from the

ENERCHEM projects of the Max Planck Society is gratefully acknowledged. Jens Weber acknowledges financial support from the German Research Foundation (DFG, Grant WE-4504/1-1).

**Supporting Information Available:** Materials and methods, synthetic procedures, and further analytical data. This material is available free of charge via the Internet at http://pubs.acs.org.

## References and Notes

(1) McKeown, N. B.; Budd, P. M. *Chem. Soc. Rev*. **2006**, *35* (8), 675–683.
(2) Ghanem, B. S.; Msayib, K. J.; McKeown, N. B.; Harris, K. D. M.; Pan, Z.; Budd, P. M.; Butler, A.; Selbie, J.; Book, D.; Walton, A. *Chem. Commun*. **2007**, *1*, 67–69.
(3) Weber, J.; Antonietti, M.; Thomas, A. *Macromolecules* **2008**, *41* (8), 2880–2885.
(4) Germain, J.; Frechet, J. M. J.; Svec, F. *J. Mater. Chem*. **2007**, *17* (47), 4989–4997.
(5) Germain, J.; Svec, F.; Frechet, J. M. J. *Chem. Mater*. **2008**, *20*, 7069–7076.
(6) Jiang, J. X.; Su, F.; Niu, H.; Wood, C. D.; Campbell, N. L.; Khimyak, Y. Z.; Cooper, A. I. *Chem. Commun*. **2008**, *4*, 486–488.
(7) Jiang, J. X.; Su, F.; Trewin, A.; Wood, C. D.; Campbell, N. L.; Niu, H.; Dickinson, C.; Ganin, A. Y.; Rosseinsky, M. J.; Khimyak, Y. Z.; Cooper, A. I. *Angew. Chem., Int. Ed*. **2007**, *46*, 8574.
(8) Weber, J.; Thomas, A. *J. Am. Chem. Soc*. **2008**, *130* (20), 6334–6335.
(9) Rose, M.; Böhlmann, W.; Sabo, M.; Kaskel, S. *Chem. Commun*. **2008**, 2462–2464.
(10) Webster, O. W.; Gentry, F. P.; Farlee, R. D.; Smart, B. E. *Makromol. Chem., Macromol. Symp*. **1992**, *54*−*5*, 477–482.
(11) Urban, C.; McCord, E. F.; Webster, O. W.; Abrams, L.; Long, H. W.; Gaede, H.; Tang, P.; Pines, A. *Chem. Mater*. **1995**, *7* (7), 1325–1332.
(12) Tsyurupa, M. P.; Davankov, V. A. *React. Funct. Polym*. **2002**, *53* (2−3), 193–203.
(13) Cote, A. P.; Benin, A. I.; Ockwig, N. W.; O'Keeffe, M.; Matzger, A. J.; Yaghi, O. M. *Science* **2005**, *310* (5751), 1166–1170.
(14) Kuhn, P.; Antonietti, M.; Thomas, A. *Angew. Chem., Int. Ed*. **2008**, *47* (18), 3450–3453.
(15) Budd, P. M.; Ghanem, B. S.; Makhseed, S.; McKeown, N. B.; Msayib, K. J.; Tattershall, C. E. *Chem. Commun*. **2004**, *2*, 230–231.
(16) Budd, P. M.; McKeown, N. B.; Fritsch, D. *J. Mater. Chem*. **2005**, *15* (20), 1977–1986.
(17) Weber, J.; Su, O.; Antonietti, M.; Thomas, A. *Macromol. Rapid Commun*. **2007**, *28* (18−19), 1871–1876.
(18) Du, N.; Robertson, G. P.; Pinnau, I.; Thomas, S.; Guiver, M. D. *Macromol. Rapid Commun*. **2009**, *30*, 584–588.
(19) Kricheldorf, H. R.; Fritsch, D.; Vakhtangishvili, L.; Schwarz, G. *Macromol. Chem. Phys*. **2005**, *206*, 2239–2247.
(20) Kricheldorf, H. R.; Lomadze, N.; Fritsch, D.; Schwarz, G. *J. Polym. Sci., Part A: Polym. Chem*. **2006**, *44*, 5344–5352.
(21) Du, N.; Song, J.; Robertson, G. P.; Pinnau, I.; Guiver, M. D. *Macromol. Rapid Commun*. **2008**, *29*, 783–788.
(22) Ghanem, B. S.; McKeown, N. B.; Budd, P. M.; Selbie, J. D.; Fritsch, D. *Adv. Mater*. **2008**, *20*, 2766–2771.
(23) Lozano-Castelló, D.; Cazorla-Amorós, D.; Linares-Solano, A. *Carbon* **2004**, *42* (7), 1233–1242.
(24) Vishnyakov, A.; Ravikovitch, P. I.; Neimark, A. V. *Langmuir* **1999**, *15* (25), 8736–8742.
(25) Dinca, M.; Long, J. R. *J. Am. Chem. Soc*. **2005**, *127*, 9376–9377.
(26) Dybtsev, D. N.; Chun, H.; Yoon, S. H.; Kim, D.; Kim, K. *J. Am. Chem. Soc*. **2004**, *126*, 32–33.
(27) As the nitrogen sorption isotherm was collected at the boiling point of nitrogen (77 K), multilayer formation and nitrogen condensation in mesopores or interparticulate voids have also to be regarded. This is different for hydrogen at 77 K and carbon dioxide at 273 K which probes micropores only.
(28) Férey, G.; Latroche, M.; Serre, C.; Millange, F.; Loiseau, T.; Percheron-Guégan, A. *Chem. Commun*. **2003**, 2976–2977.
(29) Zhao, X.; Xiao, B.; Fletcher, A. J.; Thomas, K. M.; Bradshaw, D.; Rosseinsky, M. J. *Science* **2004**, *306*, 1012–1015.
(30) Fletcher, A. J.; Thomas, K. M.; Rosseinsky, M. J. *J. Solid State Chem*. **2005**, *178*, 2491–2510.
(31) We have to note that not the complete isotherm could be fitted. We used the higher pressure regime for fitting ($p > 0.2$ bar). There are different drawbacks regarding the applicability of the Langmuir equation (hysteresis, nonuniform surface, etc.), which cannot be discussed in full detail at this stage. Calculation of the surface area assumed the molecular cross section of hydrogen to be 0.104 $nm^2$.
(32) Presumably due to the low molecular weight no mechanically stable films were formed. Brittle samples were obtained.
(33) Bos, A.; Pünt, I. G. M.; Wessling, M.; Strathmann, H. *J. Membr. Sci*. **1999**, *155* (1), 67–78.
(34) Wessling, M.; Huisman, I.; Boomgaard, T.; v., d.; Smolders, C. A. *J. Polym. Sci., Part B: Polym. Phys*. **1995**, *33* (9), 1371–1384.
(35) Wind, J. D.; Staudt-Bickel, C.; Paul, D. R.; Koros, W. J. *Ind. Eng. Chem. Res*. **2002**, *41* (24), 6139–6148.
(36) Du, N.; Robertson, G. P.; Song, J.; Pinnau, I.; Thomas, S.; Guiver, M. D. *Macromolecules* **2008**, *41*, 9656–9662.